HOSTED BY

ELSEVIER

CrossMark

Available online at www.sciencedirect.com

ScienceDirect

Progress in Natural Science: Materials International 25 (2015) 591–594

Progress in Natural Science Materials International

www.elsevier.com/locate/pnsmi
www.sciencedirect.com

Original Research

Design of optimum solid oxide membrane electrolysis cells for metals production

Xiaofei Guan[a,b,1], Uday B. Pal[a,b]

[a]Division of Materials Science and Engineering, Boston University, Boston, MA 02446, USA
[b]Department of Mechanical Engineering, Boston University, Boston, MA 02446, USA

Received 17 September 2015; accepted 30 October 2015
Available online 24 December 2015

Abstract

Oxide to metal conversion is one of the most energy-intensive steps in the value chain for metals production. Solid oxide membrane (SOM) electrolysis process provides a general route for directly reducing various metal oxides to their respective metals, alloys, or intermetallics. Because of its lower energy use and ability to use inert anode resulting in zero carbon emission, SOM electrolysis process emerges as a promising technology that can replace the state-of-the-art metals production processes. In this paper, a careful study of the SOM electrolysis process using equivalent DC circuit modeling is performed and correlated to the experimental results. A discussion on relative importance of each resistive element in the circuit and on possible ways of lowering the rate-limiting resistive elements provides a generic guideline for designing optimum SOM electrolysis cells.

Keywords: Electrolysis; Solid oxide; Membranes; Metals production; Environmentally benign

1. Introduction

Solid oxide membrane (SOM) electrolysis is an electrolytic technique for the production of metals (Me) directly from their respective oxides (MeO_x). For SOM electrolysis cells, the overall electrochemical reaction is given as

$$MeO_x \rightarrow Me + x/2\ O_2(g) \quad (1)$$

where x is the stoichiometric amount of oxygen in the metal oxide. To date, the SOM electrolysis process has been applied for the production of various technologically important metals, such as Mg, Al, Ti, Ta, Yb, and Si [1–9]. This process has also been adapted to produce alloys and intermetallics, such as Ti–Fe alloy, Ti–Si intermetallics, and $CeNi_5$ [10–13].

Fig. 1 shows a schematic illustration of a SOM electrolysis cell employing an inert oxygen anode [3]. An oxygen-ion-conducting SOM typically made of yttria-stabilized zirconia (YSZ) separates the inert anode from a molten salt (flux) electrolyte and a cathode. During electrolysis, an applied potential exceeds the dissociation potential of the metal oxide dissolved in the molten salt. The desired metal is reduced at the cathode while oxygen ions are transported through the SOM and are oxidized to pure O_2 gas at the inert anode.

2. Equivalent DC circuit

Equivalent DC circuit is a useful tool to gain an insight into the SOM electrolysis process. Fig. 2(a) presents a general equivalent DC circuit that takes into account all the known mechanisms associated with the current flow: (1) the dissociation of the desired oxide, (2) the dissociation of the impurity oxides (undesired oxides) dissolved in the flux, (3) electronic

E-mail address: upal@bu.edu (U.B. Pal).
[1]Current address: John A. Paulson School of Engineering and Applied Sciences, Harvard University, Cambridge, MA 02138, USA.
Peer review under responsibility of Chinese Materials Research Society.

http://dx.doi.org/10.1016/j.pnsc.2015.11.004

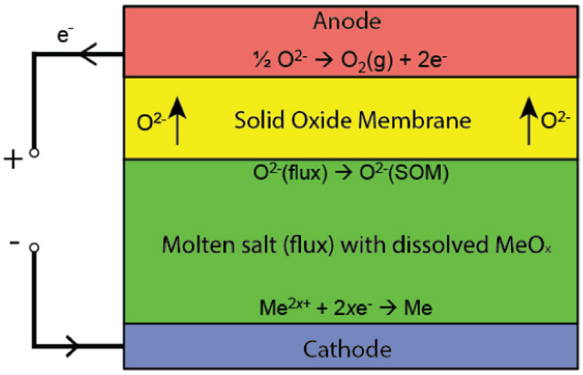

Fig. 1. Schematic illustration of a SOM electrolysis cell.

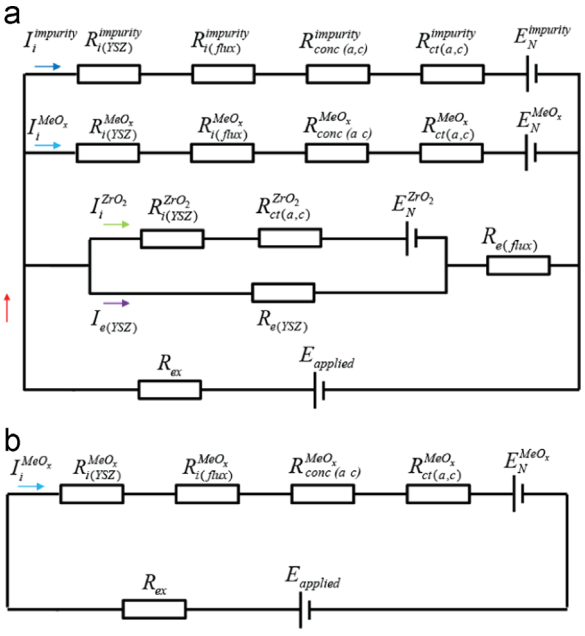

Fig. 2. Equivalent DC circuit of the SOM electrolysis cell: (a) general case and (b) ideal case.

conductivity of the flux caused by either the intrinsic electronic conductivity or the metal solubility in the flux, and (4) the various resistive contributions of the SOM [5]. The symbols used in Fig. 2 are defined in Table 1. Contributions related to the impurity oxides and the electronic conductivity of the flux are undesirable. The presence of impurity oxides in the flux can lower the purity of the metal product, and the electronic conductivity of the flux can reduce the Faradaic current efficiency for metals production. The electronic conductivity of the flux also provides a pathway for the applied potential to reduce ZrO_2 in the YSZ membrane. The issues related to impurity oxides can be mitigated by performing pre-electrolysis at lower applied potentials or through careful selection of the feed material. The issues related to the electronic conductivity of the flux needs to be mitigated by removing the sources that contribute to generating the electronic carriers or by creating an electron blocking layer around the SOM [4,14].

Table 1
Definitions of symbols in the SOM equivalent DC circuits shown in Fig. 2.

Symbol	Definition
$R_{i(YSZ)}^{impurity}$	Ionic resistance of YSZ membrane involved for impurity oxides dissociation
$R_{i(YSZ)}^{MeO_x}$	Ionic resistance of YSZ membrane involved for MeO_x dissociation
$R_{i(YSZ)}^{ZrO_2}$	Ionic resistance of YSZ membrane involved for ZrO_2 dissociation
$R_{i(flux)}^{impurity}$	Ionic resistance of flux involved for impurity oxides dissociation
$R_{i(flux)}^{MeO_x}$	Ionic resistance of flux involved for MeO_x dissociation
$R_{conc(a,c)}^{impurity}$	Concentration polarization resistance at the anode and cathode for impurity oxides dissociation
$R_{conc(a,c)}^{MeO_x}$	Concentration polarization resistance at the anode and cathode for MeO_x dissociation
$R_{ct(a,c)}^{impurity}$	Charge transfer resistance at the anode and cathode for impurity oxides dissociation
$R_{ct(a,c)}^{MeO_x}$	Charge transfer resistance at the anode and cathode for MeO_x dissociation
$R_{ct(a,c)}^{ZrO_2}$	Charge transfer resistance at the anode and cathode for ZrO_2 dissociation
$R_{e(YSZ)}$	Electronic resistance of the YSZ membrane
$R_{e(flux)}$	Electronic resistance of the flux between YSZ and bubbling tube
R_{ex}	Resistance of external lead wires and the current collectors
$E_N^{impurity}$	Nernst potential for impurity oxides dissociation
$E_N^{MeO_x}$	Nernst potential for MeO_x dissociation
$E_N^{ZrO_2}$	Nernst potential for ZrO_2 dissociation
$E_{applied}$	Applied potential
$I_i^{impurity}$	Ionic current for impurity oxides dissociation
$I_i^{MeO_x}$	Ionic current for MeO_x dissociation
$I_i^{ZrO_2}$	Ionic current for ZrO_2 dissociation
$I_{e(YSZ)}$	Electronic current passing the YSZ membrane

Fig. 2(b) shows the equivalent DC circuit for an ideal SOM cell where the circuit branches for the impurity oxides and the electronic conductivity of the flux have been removed from the general equivalent DC circuit.

3. Polarization model for an ideal SOM cell

According to the equivalent circuit shown in Fig. 2(b), $E_{applied}$ can be expressed by

$$E_{applied} = \left|E_N^{MeO_x}\right| + \eta_{ohm} + \eta_{ct(a,c)} + \eta_{conc,c} + \eta_{conc,a} \quad (2)$$

where $\left|E_N^{MeO_x}\right|$ is the absolute value of the Nernst potential for MeO_x dissociation, η_{ohm} is the ohmic polarization of the SOM cell, $\eta_{ct(a,c)}$ is the charge transfer polarization, $\eta_{conc,c}$ is the cathodic concentration polarization, and $\eta_{conc,a}$ is the anodic concentration polarization.

3.1. Ohmic polarization, η_{ohm}

Literature related to SOM electrolysis for Mg production reports that the ohmic polarization dominates the total polarization [5]. Therefore, it is critical to reduce η_{ohm} to improve

the SOM electrolysis performance. The ohmic polarization of the SOM cell is expressed as follows:

$$\eta_{ohm} = I_i^{MeO_x}\left(R_{i(YSZ)}^{MeO_x} + R_{i(flux)}^{MeO_x} + R_{ex}\right) \quad (3)$$

The η_{ohm} can be reduced by reducing the resistances of these three ohmic resistive elements, $R_{i(YSZ)}^{MeO_x}$, $R_{i(flux)}^{MeO_x}$, and R_{ex}.

The most straightforward way of reducing $R_{i(YSZ)}^{MeO_x}$ is decreasing the thickness of the YSZ membrane. Yet, reducing the thickness of the tubular YSZ membrane has a limit because it poses challenges in terms of retaining structural and mechanical integrity. Westinghouse's design of the air electrode for solid oxide fuel cells may be of interest as a replacement alternative for the YSZ tube [15]. The air electrode employs a porous one-end closed doped lanthanum manganite tube coated with YSZ film having a thickness as low as 40 μm. This can drastically decrease $R_{i(YSZ)}^{MeO_x}$. In addition to reducing the membrane thickness, the ohmic resistance can be further reduced by using higher conductivity membrane materials, such as scandia-stabilized zirconia (ScSZ), lanthanum strontium gallium magnesium oxide (LSGM), or gadolinium-doped ceria (GDC), as commonly studied in solid oxide fuel cells [16].

The $R_{i(flux)}^{MeO_x}$ can be reduced by decreasing the cell constant of the flux between the cathode and the YSZ membrane, which can be realized by reducing the distance and/or increasing the effective cross-sectional area between the cathode and the YSZ membrane. The $R_{i(flux)}^{MeO_x}$ can also be reduced by increasing the flux ionic conductivity, which can be realized by using a highly ionic conductive fluoride- or chloride-based supporting electrolytes [1,11]. Another method of increasing the flux ionic conductivity is increasing the optical basicity of the flux through adding high optical basicity oxides [17].

In terms of decreasing R_{ex}, liquid metal anode (e.g., Ag) wets YSZ membrane and contributes less to the ohmic resistance than a porous cermet anode composed of a mixture of YSZ and strontium-doped lanthanum manganite (LSM).

3.2. Charge transfer polarization, $\eta_{ct(a,c)}$

$\eta_{ct(a,c)}$ is the overpotential required to overcome the activation energy barrier for the charge transfer reactions at the electrodes. For small currents and/or rapid mass transfer, $\eta_{ct(a,c)}$ is described by the Butler–Volmer equation:

$$i = i_0 \exp\left(\frac{\alpha n \eta_{ct(a,c)} F}{RT}\right) - i_0 \exp\left(\frac{-(1-\alpha) n \eta_{ct(a,c)} F}{RT}\right) \quad (4)$$

where i_0 is the exchange current, α is the transfer coefficient, and n is the number of electrons transferred. Eq. (4) can be simplified to different forms based on each specific electrochemical system [18]. Assuming a symmetric activation energy barrier for both electrode reactions, the value of α is suggested to be 0.5. Therefore, from Eq. (4), $\eta_{ct(a,c)}$ can be expressed by Eq. (5). Detailed derivation can be found elsewhere [19].

$$\eta_{ct(a,c)} = \frac{RT}{xF} \ln\left[\left(\frac{I_i^{MeO_x}}{2i_0}\right) + \sqrt{\left(\frac{I_i^{MeO_x}}{2i_0}\right)^2 + 1}\right] \quad (5)$$

The charge transfer resistance, $R_{ct(a,c)}^{MeO_x}$, is the differential of the $\eta_{ct(a,c)}$ with respect to $I_i^{MeO_x}$, as expressed by

$$R_{ct(a,c)}^{MeO_x} = \frac{d\eta_{act}}{dI_i^{MeO_x}} = \frac{RT}{xF} \frac{1}{\sqrt{\left(I_i^{MeO_x}\right)^2 + (2i_0)^2}} \quad (6)$$

Eq. (6) suggests that $R_{ct(a,c)}^{MeO_x}$ can be reduced by increasing the exchange current, i_0. Supposing the electrode areas to be constant, i_0 is a measure of the electrocatalytic activity of the electrodes for the electrochemical reactions involved. Literature reports have shown that the charge transfer reaction ($O^{2-} \rightarrow 1/2O_2(g) + 2e^-$ or $H_2(g) + O^{2-} \rightarrow H_2O\ (g) + 2e^-$) at the liquid metal electrode is rapid [20–22]. Therefore, the value of i_0 is limited by the metal reduction reaction ($Me^{2x+} + 2xe^- \rightarrow Me$) at the cathode. To achieve a high cathodic i_0, the selected cathode material must have a high catalytic activity for the desired metal reduction reaction. Second, the cathode surface roughness can be improved to provide more reaction sites. Third, the concentration of metal ions at the cathode must be maintained high employing sufficient stirring.

3.3. Cathodic concentration polarization, $\eta_{conc,c}$

$\eta_{conc,c}$ is the overpotential resulting from the MeO_x (or Me^{2x+}) concentration gradient across the diffusion layer at the cathode surface, and it is expressed by the following equation, where $i_{l,c}$ is the cathodic limiting current [5]:

$$\eta_{conc,c} = \frac{RT}{2xF} \ln\left(\frac{i_{l,c}}{i_{l,c} - I_i^{MeO_x}}\right) \quad (7)$$

The cathodic concentration resistance, $R_{conc(c)}^{MeO_x}$, is the differential of $\eta_{conc,c}$ with respect to $I_i^{MeO_x}$, as expressed by

$$R_{conc(c)}^{MeO_x} = \frac{d\eta_{conc,c}}{dI_i^{MeO_x}} = \frac{RT}{2xF} \frac{1}{i_{l,c} - I_i^{MeO_x}} \quad (8)$$

Eq. (8) indicates that $R_{conc(c)}^{MeO_x}$ can be reduced by increasing $i_{l,c}$, which can be realized by increasing the mass diffusivity of MeO_x in the flux, increasing the bulk concentration of MeO_x in the flux, and/or decreasing the diffusion layer thickness through stirring.

3.4. Anodic concentration polarization, $\eta_{conc,a}$

$\eta_{conc,a}$ is the overpotential resulting from the oxygen concentration gradient across the diffusion layer at the anode surface. The $\eta_{conc,a}$ has different expressions depending on the anode material and configuration. In the case of liquid Ag anode for pure O_2 evolution, the liquid Ag is saturated with oxygen as it is in equilibrium with the oxygen in the environment. Instead of gradual diffusion of oxygen in the liquid Ag, the oxygen forms bubbles at the Ag/YSZ interface and leaves the liquid silver, so the oxygen partial pressure at the Ag/YSZ interface for bubble formation ($P_{O_2(Ag)}^{bf}$) must exceed the atmospheric pressure (1 atm). The difference in the oxygen partial pressure results in an overpotential that must be exceeded to form oxygen bubbles [5]. Then, the $\eta_{conc,a}$ is

expressed by

$$\eta_{conc,a} = \frac{RT}{2xF} \ln\left(\frac{P^{bf}_{O_2(Ag)}}{1\ \text{atm}}\right) \tag{9}$$

Typically, the value of $P^{bf}_{O_2(Ag)}$ falls in the range of 1–2 atm, and therefore the value of $\eta_{conc,a}$ is less than 0.1 V, which is negligibly small compared to other polarizations [5]. This indicates liquid Ag is an excellent anode for reducing anodic concentration polarization.

In the case of liquid metal (Ag, Sn, or Cu) anode stirred by fuels such as H_2 or CH_4, the oxygen partial pressure in the bulk of the liquid metal anode is determined by the fuel used. Instead of forming oxygen bubbles, the oxygen diffuses across a boundary layer near the liquid metal/YSZ interface and reacts with the fuel. Expression of $\eta_{conc,a}$ is shown as follows where b is the boundary layer thickness in the liquid metal anode, $D_{[O]}$ is the diffusivity of dissolved oxygen in the liquid metal anode, and $C^o_{[O]}$ is the bulk concentration of dissolved oxygen in the liquid metal anode [19].

$$\eta_{conc,a} = \frac{RT}{2xF} \ln\left(1 + \frac{b}{2xFAD_{[O]}C^o_{[O]}} I_i^{MeO_x}\right) \tag{10}$$

Accordingly, the anodic polarization resistance is expressed as follows:

$$R^{MeO_x}_{conc(a)} = \frac{d\eta_{conc,a}}{dI_i^{MeO_x}} = \frac{RT}{2xF} \ln\left(\frac{1}{\frac{2xFAD_{[O]}C^o_{[O]}}{b} + I_i^{MeO_x}}\right) \tag{11}$$

This expression indicates that the $R^{MeO_x}_{conc(a)}$ can be reduced by decreasing b, which can be realized by increasing the stirring rate of the fuel.

3.5. Total cell resistance, $R^{MeO_x}_{Total}$

In summary, in the case of liquid Ag anode for pure O_2 evolution, the total cell resistance ($R^{MeO_x}_{Total}$) of a SOM electrolysis cell for dissociating MeO_x is expressed by

$$R^{MeO_x}_{Total} = R_{i,ohm} + R^{MeO_x}_{ct(a,c)} + R^{MeO_x}_{conc(c)} = \left(R^{MeO_x}_{i(YSZ)} + R^{MeO_x}_{i(flux)} + R_{ex}\right) + \frac{RT}{xF} \frac{1}{\sqrt{\left(I_i^{MeO_x}\right)^2 + (2i_0)^2}} + \frac{RT}{2xF} \frac{1}{i_{l,c} - I_i^{MeO_x}} \tag{12}$$

In the case of liquid metal anode stirred by fuels, another term for $R^{MeO_x}_{conc,a}$ needs to be added, and the expression of $R^{MeO_x}_{Total}$ is shown as follows:

$$\begin{aligned} R^{MeO_x}_{Total} &= R_{i,ohm} + R^{MeO_x}_{ct(a,c)} + R^{MeO_x}_{conc(c)} + R^{MeO_x}_{conc(a)} \\ &= \left(R^{MeO_x}_{i(YSZ)} + R^{MeO_x}_{i(flux)} + R_{ex}\right) + \frac{RT}{xF} \frac{1}{\sqrt{\left(I_i^{MeO_x}\right)^2 + (2i_0)^2}} \\ &\quad + \frac{RT}{2xF} \frac{1}{i_{l,c} - I_i^{MeO_x}} + \frac{RT}{2xF} \ln\left(\frac{1}{\frac{2xFAD_{[O]}C^o_{[O]}}{b} + I_i^{MeO_x}}\right) \end{aligned} \tag{13}$$

To design an optimum SOM electrolysis cell, each of these resistances needs to be lowered and optimized, as discussed above. The feasibility of this model has also been demonstrated for a SOM electrolysis cell for the dissociation of MgO into Mg and O_2(g) [5]. For specific SOM electrolysis experiment, each term in the general expression of the total resistance can be quantified using curve-fitting. Based on the results, the rate-limiting resistive elements can be identified and improved.

4. Conclusions

In this letter, an equivalent DC circuit modeling of the SOM electrolysis process is presented. The explicit expression of each resistive element of an ideal SOM cell provides direct information on how to lower the rate-limiting elements, and thus will provide generic guideline for designing optimum SOM electrolysis cells and beyond.

Acknowledgment

The authors would like to thank Dr. Adam C. Powell IV for helpful discussion. The material is based on work supported by the Department of Energy (DE-FC36-14GO14011; DE-EE0003454; and DE-EE0005547) and the National Science Foundation (DMI-9424069; DMI-0457381; CBET-1210442; and DMR-08-19762).

References

[1] U.B. Pal, D.E. Woolley, G.B. Kenney, JOM 53 (2001) 32–35.
[2] A. Krishnan, U.B. Pal, X.G. Lu, Metall. Mater. Trans. B 36B (2005) 463–473.
[3] X. Guan, U.B. Pal, S. Gopalan, A.C. Powell, J. Electrochem. Soc. 160 (2013) F1179–F1186.
[4] E. Gratz, X. Guan, J. Milshtein, U.B. Pal, A.C. Powell, Metall. Mater. Trans. B 45 (2014) 1325–1336.
[5] X. Guan, U.B. Pal, A.C. Powell, Metall. Mater. Trans. E 1 (2014) 132–144.
[6] S. Su, X. Guan, U.B. Pal, Proceedings of the TMS Annual Meeting & Exhibition, Orlando, FL, 2015.
[7] M. Suput, R. DeLucas, S. Pati, G. Ye, U. Pal, A. Powell, Min. Proc. Extr. Met. 117 (2008) 118–122.
[8] A. Krishnan, X.G. Lu, U.B. Pal, Scand. J. Met. 34 (2005) 293–301.
[9] Y. Jiang, J. Xu, X. Guan, U.B. Pal, S.N. Basu, Mater. Res. Symp. Proc. 1493 (2013) 231–235.
[10] X. Lu, X. Zou, C. Li, Q. Zhong, W. Ding, Z. Zhou, Metall. Mater. Trans. B 43 (2012) 503–512.
[11] B. Zhao, X. Lu, Q. Zhong, C. Li, S. Chen, Electrochim. Acta 55 (2010) 2996–3001.
[12] X. Zou, X. Lu, C. Li, Z. Zhou, Electrochim. Acta 55 (2010) 5173–5179.
[13] X. Zou, X. Lu, Z. Zhou, C. Li, W. Ding, Electrochim. Acta 56 (2011) 8430–8437.
[14] X. Guan, S. Su, U.B. Pal, A.C. Powell, Metall. Mater. Trans. B. 45 (2014) 2138–2144.
[15] S.C. Singhal, Solid State Ionics 152–153 (2002) 405–410.
[16] S.M. Haile, Acta Mater. 51 (2003) 5981–6000.
[17] K. Mills Southern African Pyrometallurgy, Misty Hills, South Africa, 2011.
[18] S. Pati, K.J. Yoon, S. Gopalan, U.B. Pal, Metall. Mater. Trans. B. 40B (2009) 1041–1053.
[19] X. Wei, X. Jin, Y. Deng, D. Wang, G.Z. Chen, Chem. Eur. J. 13 (2007) 604–612.
[20] K.E. Oberg, L.M. Friedman, W.M. Boorstein, R.A. Rapp, Metall. Trans. 4 (1973) 75–82.
[21] S. Yuan, U.B. Pal, K.C. Chou, J. Electrochem. Soc. 141 (1994) 467–474.
[22] P. Soral, U.B. Pal, H.R. Larson, B. Schroeder, Metall. Mater. Trans. B. 30B (1999) 307–321.